3
Fabrication and Characterization Processes

This chapter reveals the description related to experimental techniques and characterization processes that are used in this thesis. These techniques and processes were utilized to design and characterize the AlGaN/GaN HEMT device and its applications in heavy metal ions sensing. Herein, a brief theoretical overview of the fabrication and characterization processes are explained. In this context, this chapter is divided into two sections in which the first one illustrates different fabrication techniques such as MOCVD, thermal evaporation, sputtering, and optical lithography used for the development of AlGaN/GaN HEMT and in another section various structural and surface morphological process like XRD (X-ray diffraction), AFM (atomic force microscopy), FESEM (field emission scanning electron microscopy), and Raman spectroscopy, as well as electrical characterization, is explained.

3.1 FABRICATION PROCESSES

3.1.1 Metal-Organic Chemical Vapor Deposition (MOCVD)

Two growth techniques widely used for III-N growth are MOCVD and Molecular Beam Epitaxy (MBE). The MOCVD technique was derived at North American Rockwell in 1968 and become a dominating technique in the researches related to the growth of compound semiconductor materials and devices [Liddle, 2008]. Nowadays, it has become an important technique due to ever increase industrial demand in the various applications of III-N semiconductors in the past few decades.

The MOCVD is a nonequilibrium growth process in which the transportation of precursor materials and successive reactions of group-III alkyls and group-V hydrides happens in a heated region. There are three major sections in a typical MOCVD system: the gas transport system, the reaction chamber, and the reaction protection system [Liddle, 2008]. Here, the gas mixtures comprise the essential molecules known as precursors for the epitaxial growth of the desired materials. In general, the growth of III-N semiconductors in the MOCVD is carried out using the hydride and alkyl precursors. Currently, hydrogen is utilized as carrier gas because of its purity. In the system, the growth temperature generally keeps around 550°C -1100°C to obtain a stable growth rate as well as high-quality epi layers [Jha, 2007]. GaN films showed their best electrical and optical properties at the growth temperature of 1050 °C [Bhat *et al.*, 2014; Liddle, 2008]. Furthermore, the substrate temperatures over 1100 °C can initiate the formation of defects in the GaN layer; hence, the perfect control of the temperature in this range is highly desirable [Pearton, 2000]. In the MOCVD, the growth rate can be easily controlled by adjusting the flow rate of the precursors along with the slight change in reactor temperature and pressure. In addition, the composition and growth rates can be further controlled by dilution of different elements of the gas flow [Jha, 2007].

In this thesis work, the growth of epilayer of AlGaN/GaN HEMT was carried out on Si (111) substrate under the collaborative work between IIT Jodhpur and Institute of Materials Research and Engineering (IMRE), Agency for Science, Technology and Research (A*STAR), Singapore. Under this collaboration, the AlGaN/GaN HEMT epilayers were grown on Si (111) substrate by AXITRON CCS 19×2-inch MOCVD system, refurbished at IMRE, A*STAR, Singapore. The scientists of IMRE, A*STAR Singapore, have performed the epitaxial growth of

AlGaN/GaN HEMT on Si (111). Further details related to the growth of AlGaN/GaN epilayers will be discussed in chapter 4. Moreover, the author performed the device fabrication and development of the sensors at the IIT Jodhpur.

3.1.2 Thermal Evaporation

Thermal evaporation is a well-known technique for thin-film deposition of metals in the microfabrication in which the evaporation of metals is performed in a high vacuum. This high vacuum is of the order of 10^{-6} mbar, which provides the metal vapor particles a long mean free path so that they can travel to the sample or substrate without collision of other particles or gases and can condense back to the solid form. The schematic of the thermal evaporation system is shown in Figure 3.1. The evaporation system work on the principle of resistive heating. In the thermal evaporation process, a resistive filament or boat is utilized, which contains the metal wire or small metal chunks of the particular metal to be evaporated. These boats or filaments are made by metals having high melting points such as tungsten and molybdenum. In order to perform the thermal evaporation process, a large current is passed through the boat or filament under a high vacuum. The crystal thickness monitor continuously monitors the thickness of the metal film on the sample. During the process of deposition, the sample rotation usually provides the uniform deposition of the metal layer on each sample.

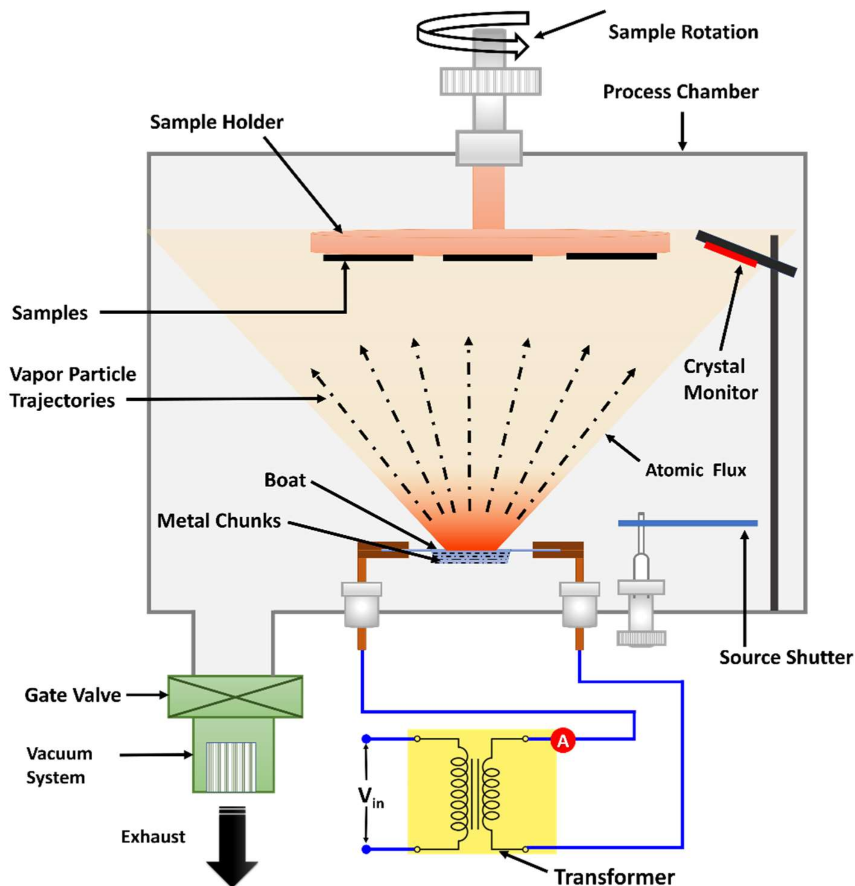

Figure 3.1: Schematic of the thermal evaporation system

Figure 3.2 depicts the system utilized in this work for the thermal evaporation of metals. This system is operated in the microelectronics lab of IIT Jodhpur. This system is a three-boat thermal evaporation system in which three metals can be evaporated and deposited on the sample without breaking the vacuum. By using this system, there were three metals, Aluminium

Figure 3.2: Thermal evaporation system at Microfabrication lab, IIT Jodhpur

(Al), Chromium (Cr), and Gold (Au) deposited on the device, which was further utilized for source contact formation. The evaporation of metals is performed by applying a high current (more than 80 A) to evaporate metals. In this system, the turbomolecular pump is used for high vacuum creation. Also, a chiller unit is used for making the system cool during the evaporation process.

3.1.3 RF Sputtering

RF (Radio Frequency) sputtering is the most common deposition technique, widely used for the deposition of insulating materials as well as metal-oxides. This method provides several befits such as low-temperature deposition, good adhesiveness of the materials over substrates or samples.

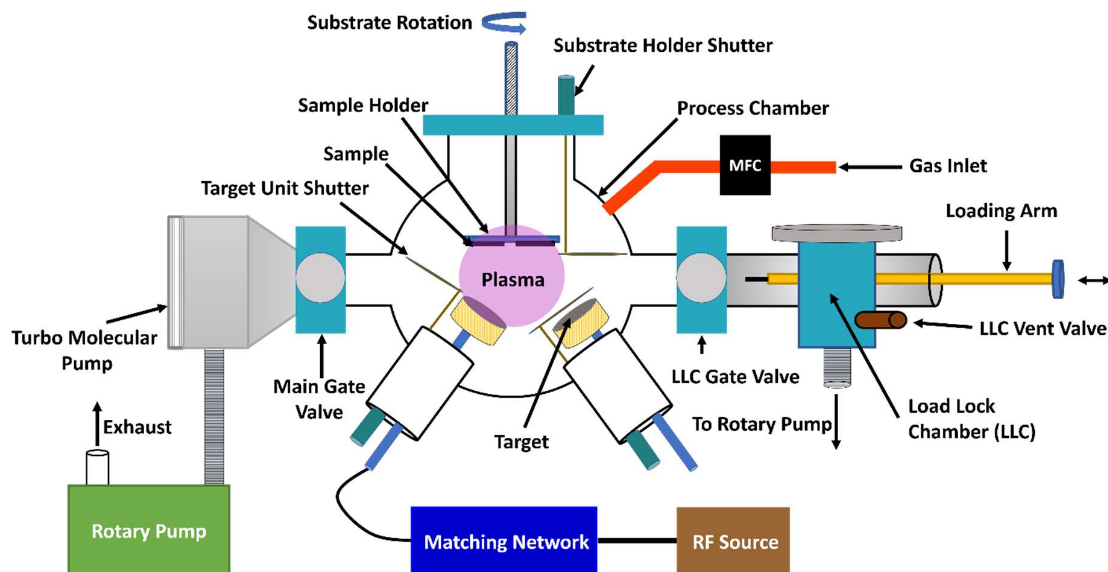

Figure 3.3: Schematic representation of the RF sputtering system

The sputtering process is carried out in a high vacuum similar to the thermal evaporation process. Figure 3.3 shows a schematic of the general RF sputtering system. In this system, a high-frequency alternating voltage of 13.56 MHz has been utilized in RF sputtering systems and can be capacitively coupled through a target of insulating material to the plasma [Plummer *et al.*, 2012]. The frequency of RF power should be sufficiently high to maintain a continuous plasma, and It should also be higher than the system's effective RC time constant [Plummer *et al.*, 2012]. For typical RF-frequency power supplies, an impedance matching network is also required. For a typical RF power source, an impedance matching network is also necessary to provide RF power to the sputtering target and hence is added in conjunction with the RF power supply. A pallet of particular material required to deposit on the substrate is called target in the sputtering system. This target is mounted on an RF magnetron and connected to an RF power supply. The sputtering system used in this work has the load-lock assembly, by which the samples have been inserted and removed to/from the process chamber by a rod called loading arm. It helps to maintain the vacuum of the process chamber. After loading the samples, the vacuum process is started in order to reduce the possible contamination during the sputtering process. In order to achieve a high vacuum in the process chamber, the rotary pump afterward turbomolecular pump is utilized. The carrier reactive gases are inserted in the processing chamber by mass flow controller (MFC), which provides a constant flow of these gases to the chamber. Similar to the thermal evaporation system, the substrate rotation is utilized to obtain a uniform thickness of the thin film of the desired material on the sample.

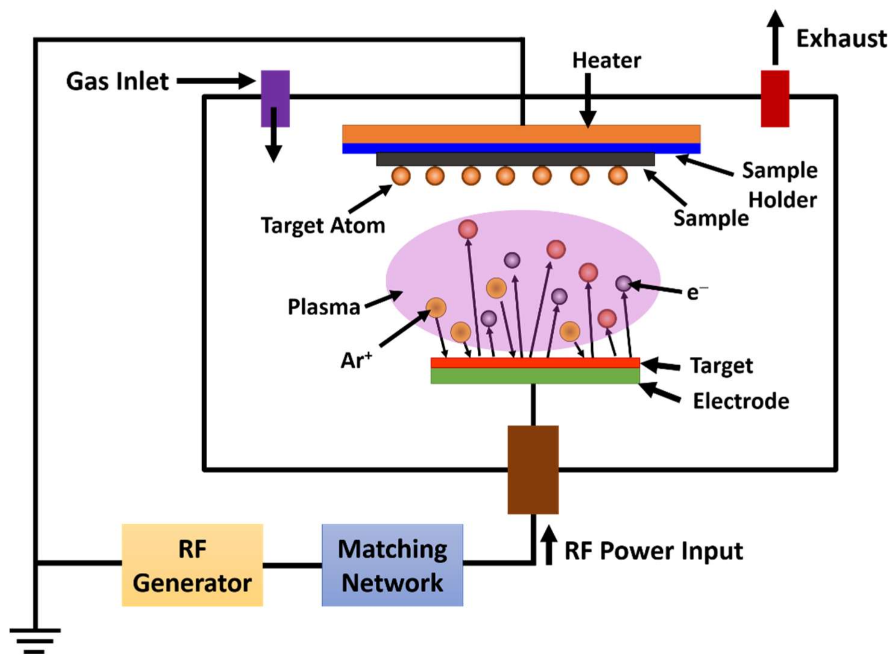

Figure 3.4: Illustration of the RF sputtering process

Figure 3.4 explains the RF sputtering mechanism. Once the system reaches enough high vacuum (in 10^{-6} mbar), inert gas or the mixture of inert and reactive gas is inserted in the process chamber, and desirable gas pressure is maintained. Furthermore, the inserted gas is ionized by an appropriate voltage between the target and substrate and generates discharge called plasma. While applying the larger electric field between the target (cathode) and the sample (anode), these ions become accelerated and attracted by the cathode. When these accelerate ions strike the target surface (cathodic surface), they transfer their energy to the surface atoms and eject them by the continuous bombardment of the target. These dislodged target atoms were then get deposited on the anodic substrate or sample surface. In this process, the inert gas (Argon here) creates a thin film of the same composition of the target material, whereas the mixture of the inert and reactive

gases such as Nitrogen can deposit a thin film of the product of the reaction between the sputtered atoms and reactive gas. In addition, the secondary electrons are also emitted during the ion bombardment apart process, which can help to sustain the plasma [Plummer *et al.*, 2012].

Figure 3.5 depicts a pictorial representation of the RF sputtering system utilized in this thesis for the fabrication process at the microfabrication laboratory IIT Jodhpur. By using this system, several parameters were utilized, such as RF power, deposition time, the distance between target and substrate, flow rates of gases, and process chamber pressure to observe the quality of thin film with optimum thickness. The structural, optical, and surface morphological properties of the thin film can be varied by variation in these parameters.

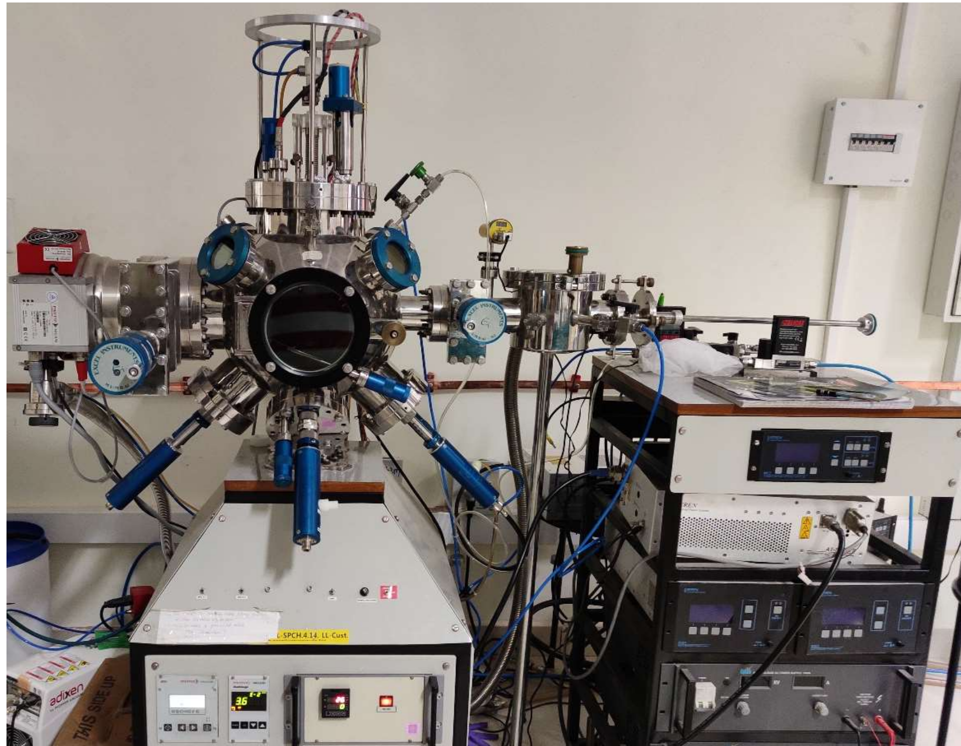

Figure 3.5: Photograph of the sputtering system at microfabrication lab, IIT Jodhpur

3.1.4 Lithography

Lithography is an important technique in the microfabrication processes in which the patterns available at the mask is transferred to a thin layer of photoresist, coated on the surface of the substrate. Generally, there are two types of lithography techniques used: optical lithography and electron beam or-beam lithography. In this work, optical lithography is utilized to develop AlGaN/GaN HEMT devices as it is a fast process; however, it requires alignment accuracy.

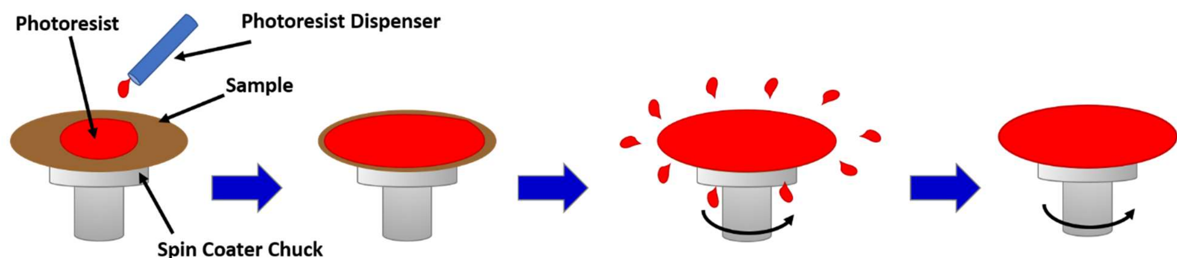

Figure 3.6: Illustration of Spin coating process [Acar, 2009]

Optical lithography is also called photolithography, in which a radiation-sensitive compound to UV light known as *photoresist* is utilized for pattern formation. Photolithography is a multi-step process that involves several process steps such as photoresist coating, soft-baking, mask alignment, exposure to UV light, development of the photoresist, the *post-exposure bake* (PEB) or the hard-bake, etching or lift-off and removal of photoresist [Plummer *et al.*, 2012]. The samples used for the pattering process were coated by photoresist using the spin coating technique. The working of the spin coating technique is explained in Figure 3.6. Initially, the sample is kept on the vacuum chuck of the spin coater, then a particular amount of photoresist is dispensed on the sample, which is spread over it. After this, the spin coater rotates at the desired speed for a particular time to coat the sample by photoresists. In this work, a programmable spin coater is used for photoresist coating on the sample and is shown in Figure 3.7. This spin coating system is installed in our microfabrication laboratory at IIT Jodhpur. Depending upon the thickness requirement of the photoresist, the rotation speed as well the time is optimized.

Figure 3.7: Photograph of the spin coating system, installed at IIT Jodhpur

After coating the photoresist on the sample, the sample is soft baked on the hot plate at $100^{o}C$ for 60 s to evaporate the solvents from the sample. In the next step, a well-patterned chrome coated quartz photomask is employed to expose the particular area on the surface of the sample. Furthermore, the alignment process is carried out using alignment marks available on the mask and the sample to match the pattern at the mask, along with the previously developed pattern on the sample. The correct alignment of these alignment marks is crucial for fabrication yield. In this work, the Karl Suss MJB-4 mask aligner system has been utilized for alignment and exposure and has shown in Figure 3.8. This system has two UV exposure modes, mainly contact exposure (soft, hard, vacuum) and proximity printing or gap contact mode. In this work, the soft contact mode has been utilized for the patterning process.

In the photolithography process, two types of photoresists are used: positive photoresist and negative photoresists, which can be discriminated by their behavior under UV exposure. The positive photoresists are photo solubilize in nature, i.e., the exposed regions under UV is become more soluble in developer solutions and easily removed during the process and hence the same patterns made in the positive resist as patterned on the mask. Whereas in negative photoresists, the exposed regions under UV have become hard than unexposed resists. This unexposed resist was then removed, and exposed resist remains on the sample; hence the patterns formed on the sample are just reverse than that of the mask patterns [Van Zant, 2013]. In this work, the positive photoresist S1813 was used for patterning of the AlGaN/GaN HEMTs, which is developed in

CD-26 developer solution after UV exposure. Figure 3.9 shows the pictorial explanation of the patterning process using positive photoresists. In this figure, the UV exposure and development of the positive photoresist are summarized.

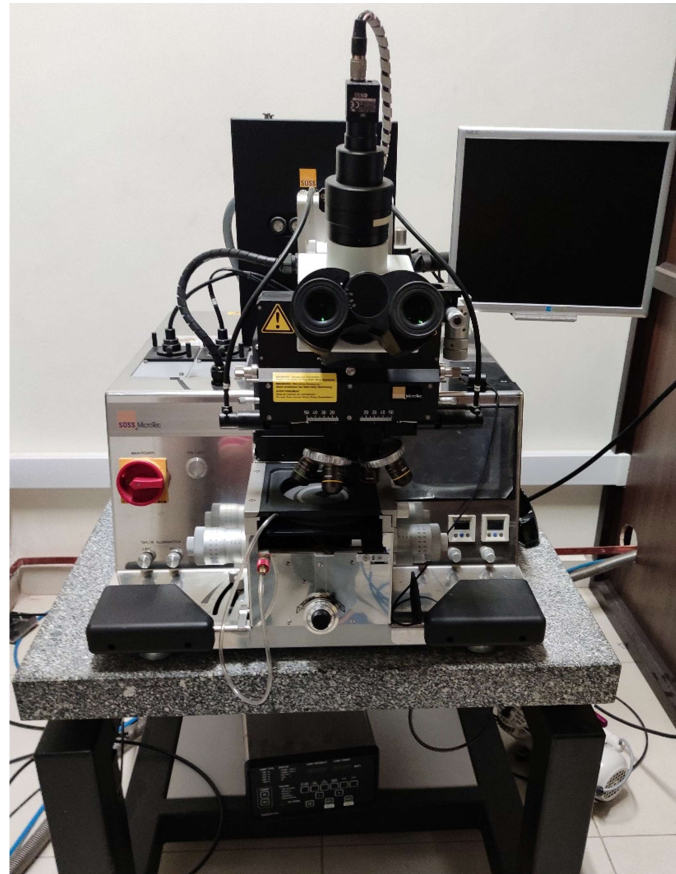

Figure 3.8: Image of MJB-4 mask aligner system at microfabrication lab, IIT Jodhpur.

After the development of the photoresist, the samples go through the hard bake treatment. Hard-baking or post-exposure bake is performed for heating the samples at 110 °C for 3 minutes using a hot plate. It is employed to harden the photoresist by further evaporating any remaining residue of the solvents of the photoresists and the developer. Besides, it also improves the adhesiveness of the resist to the surface of the sample.

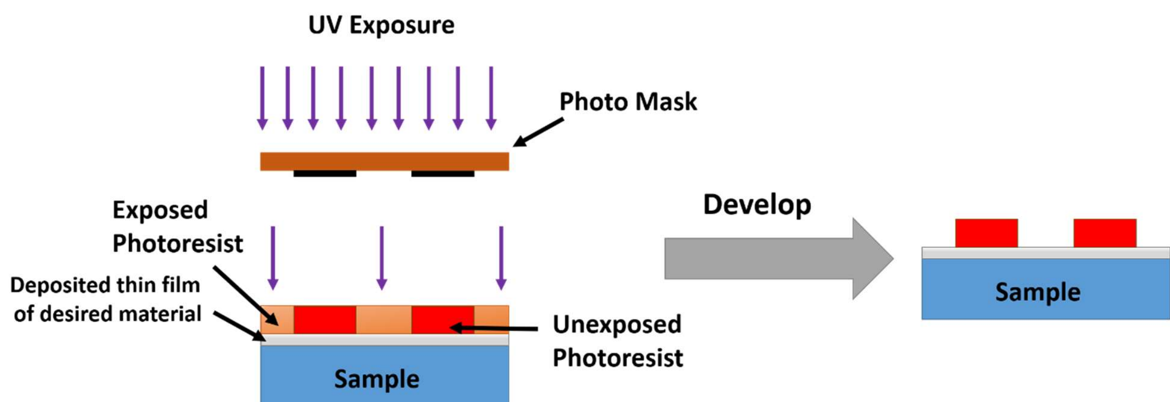

Figure 3.9: Pictorial illustration of exposure and development process using positive photoresist.

After the post-exposure baking process, the etching process was carried out using dry or wet etching techniques. In the etching process, the particular etchant is utilized to remove the material from selected places. Here the material can be metal, semiconductor, or insulator type. In this work, the wet etching process has been carried out to remove the metals and insulators from the desired places. The etching process is explained step by step in Figure 3.10.

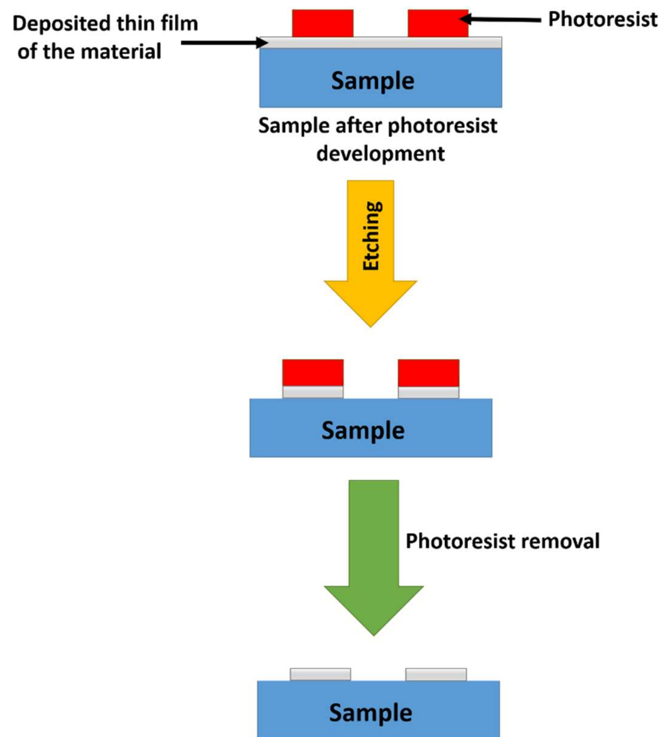

Figure 3.10: Schematic description etching process.

After the competition of the etching process, the photoresist is completely removed from the sample by various resist removal solvents. However, in this wok, acetone (CH_3COCH_3) is utilized to remove both positive photoresists.

3.2 CHARACTERIZATION PROCESSES

In this work, there were many characterization processes utilized to determine the device behavior as well as for sensor performance. The descriptions of these processes are given as follows.

3.2.1 X-Ray Diffraction

X-ray diffraction (XRD) is the most common process to analyze various structural properties such as composition, crystal orientation, and phase of the material. The X-ray diffraction determines the structure information of the material, including the lattice parameters and the grain size. Figure 3.11 shows the schematic illustration of X-ray diffraction. Here, the generation of X-rays is carried out by cathode-ray tubes, which contains Cu-Ka as a radiation source as copper is the most common target material. This Cu-Ka radiation source generates the X-ray of the wavelength of 1.54 Å, passes through the filters to monochromatic X-ray radiation, and is directed towards the samples by passing through the collimator. The sample is further scanned through the 2θ angles range, which observes all possible diffraction peaks related to the lattice structure. The diffracted X-rays are then detected and processed by the X-ray detector [Cullity, 2018].

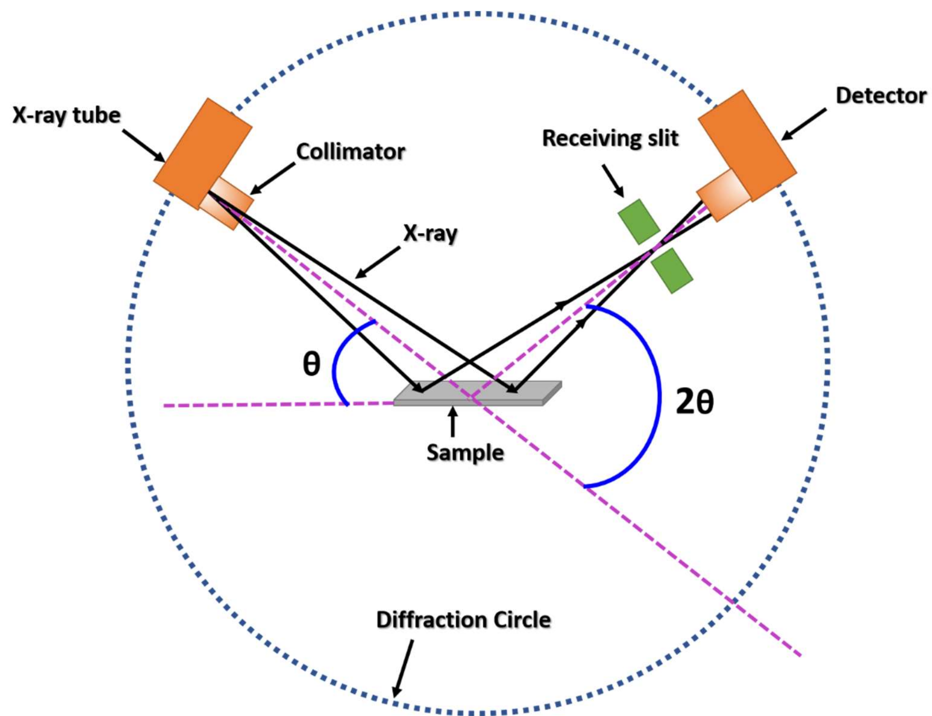

Figure 3.11: Schematic illustration of X-ray diffraction

The X-ray diffraction principle is based on the constructive interference of monochromatic radiation of X-rays and crystalline planes of the samples. This constructive interference can be observed by satisfying Bragg's law, which can be given as:

$$n\lambda = 2d\ sin\theta \tag{3.1}$$

where n is the order of diffraction, d is the lattice spacing, λ is the wavelength of the X-rays, and θ is the angle of diffraction. For constructive interference, the value of n=1 for constructive interference [Pillai, 2015]. Figure 3.12 illustrates Bragg's law of diffraction. Bragg's law explains the relation between the angle of diffraction angle and the lattice spacing in a crystalline sample using the incident ray of a particular wavelength. By the above expression, the values of lattice spacing d can be calculated by the parameters n, θ, and λ.

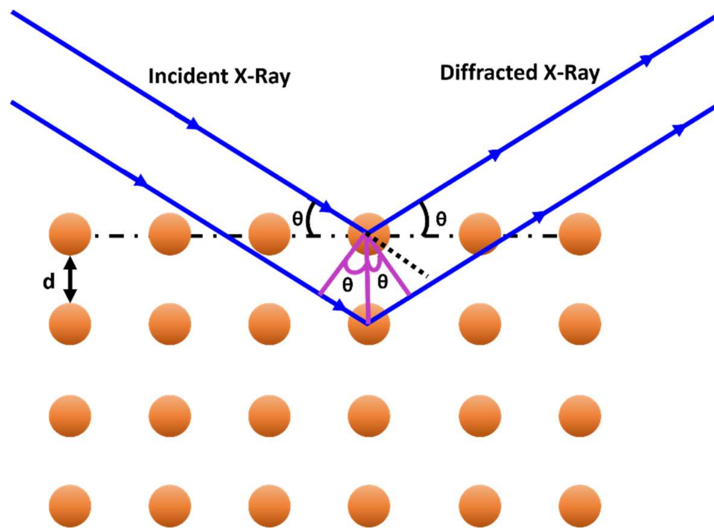

Figure 3.12: Explanation of Bragg's law for X-ray diffraction.

The obtained X-ray diffraction (XRD) data can be compared with Joint Committee Powder Diffraction Standards (JCPDS) in order to identify the unknown material. The X-ray diffraction has been performed here using the Bruker XRD system (D8 Advance) and is shown in Figure 3.13.

Figure 3.13: X-ray diffraction system (D8 Advance, Bruker) at IIT Jodhpur.

3.2.2 Atomic Force Microscopy

The Atomic Force Microscopy (AFM) is the most suitable technique for the nanoscale surface study of the samples. The application of different attractive or repulsive forces like dipole-dipole, electrostatic, magnetic, and Van-Der-Waal forces between the probe and sample allows for the detection of various mechanical properties three-dimensional topography of the sample's surface. Figure 3.14 shows the schematic setup of the AFM. Here, a cantilever having a sharp tip is mounted over the sample. The oscillation and z plane movement of the cantilever is enabled by the piezo-element, whereas the piezo motor controls the XY-plane movement of the sample. When the cantilever tip interacts with the sample, the deflection in the cantilever can be observed because of forces between tip and sample surface. The deflection of the cantilever is measured by the change in the reflection of the laser positioned at the back of the cantilever. A photodiode detects this change in the laser by showing variation in photocurrent.

The AFM generally works in three modes: contact mode, non-contact, and tapping mode [Zhang *et al.*, 2008]. In the contact mode, the measurement of the surface profile is performed by the deflection of the cantilever after forcing it directly on the surface at a particular force. Here, the cantilevers with low stiffness with a low spring constant are utilized to avoid the sample's damage. In non-contact mode, the cantilever is put at a particular height above the sample and vibrates at a certain frequency along with a small amplitude.

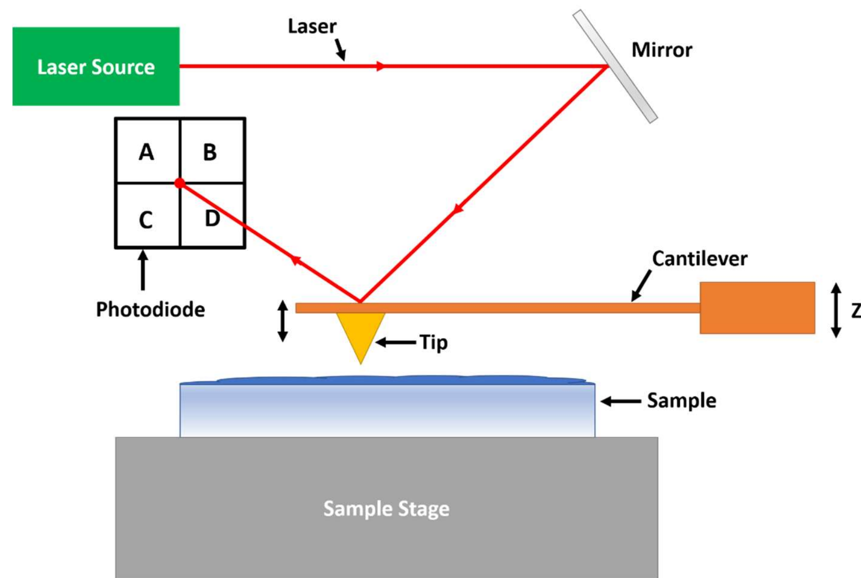

Figure 3.14: Schematic setup of Atomic Force Microscopy (AFM)

When the tip associated with the cantilever arrives in proximity to the surface of the sample, i.e., in the Van-der-Waal force range, a repulsive force comes into the picture to make it away from the sample, whereas if the tip goes far away from the sample, the attraction force brings the tip back in the range of Van-der-Waal force. Hence, the variation in the height profile of the sample can introduce attraction or repulsive forces between the probe and the sample and causes the deflection of the cantilever. In the tapping mode or intermittent mode, the cantilever is vibrated near the resonance frequency. The contact of the cantilever with the sample happens only at the bottom of the amplitude of the resonant frequency. The interactive forces, i.e., attraction and repulsion forces between the surface and the tip at the proximity, can deflect the cantilever, and hence the oscillation varies. Generally, the tapping mode produced a lesser amount of damage to the surface than contact mode as the forces applied on the surface of the sample for a very short period and sideways forces are sufficiently lower [Mehlhose, 2019]. By employing an electronic feedback control system in each mode, the position of the AFM tip can be continuously monitored and sustained over the surface. Hence, the continuous monitoring of the distance between sample and tip by photodetector using tracing and retracing process and the feedback system provides the electrical signal at each x-y point that helps to the scanning software to construct the sample morphology at nanometer scale range. Figure 3.15 shows the pictorial view of the AFM system in IIT Jodhpur.

Figure 3.15: Pictorial view of Atomic Force Microscopy (AFM)

3.2.3 Field Emission Scanning Electron Microscopy

Field Emission Scanning Electron Microscopy (FESEM) is a very effective instrument for analyzing surface morphology, including the size and shape and the thickness monitoring of the nanostructures on the surface. Further, the high-resolution imaging of the nanostructures also possible. The working of FESEM is similar to the scanning electron microscopy (SEM) as it provides detailed information on the surface of the sample by imaging except for much higher resolution and broad energy range. Also, the use of an electron gun principally distinguishes the FESEM and SEM systems. The FESEM uses a field emission gun that offers enormously focused, high and low-energy electron beams that increase spatial resolution. It also provides to work at low potentials (0.02–5 kV), which effectively reduces the charging effect on non-conducting samples [Zhang *et al*., 2008].

The principle of FESEM depends upon the interaction of the incident electrons over the atoms of a particular sample, which produce backscattered and secondary electrons, which are very helpful for sample imaging [Zhang *et al*., 2008]. Both the electron types are beneficial in the complete morphological analysis of the sample as the backscattered electrons provide the information related to dissimilarities in the composition of the multiphase samples. The secondary electrons illustrate the morphological and topographical behavior of the surface of the sample.

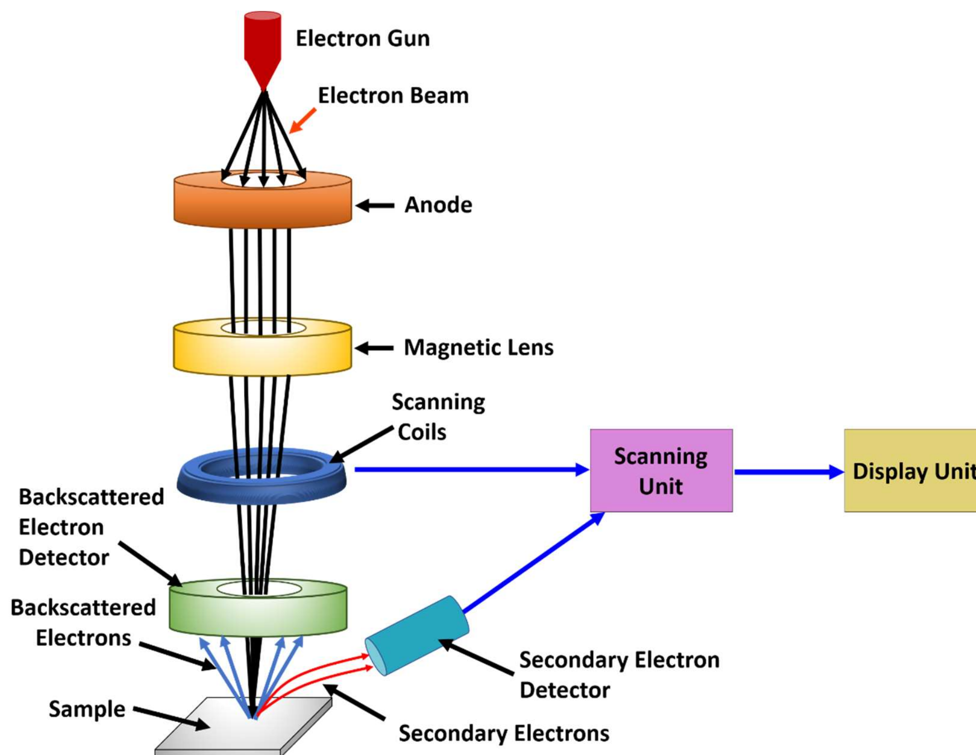

Figure 3.16: Schematic illustration and working of FESEM

Figure 3.16 shows the working of FESEM. Here, the field emission gun generates the electrons of high energy in a high vacuum. Then the field gradient accelerates these electrons, which helps them to pass from the different electromagnetic lenses. These lenses focused on the sample. After the interaction of these electrons to the atoms of the sample's surface, the secondary and backscattered electrons generated, which were then collected to their specific detectors and processed to the scanning system. In the FESEM, the raster scanning is performed for the imaging [Zhang *et al*., 2008]. In this work, the FESEM was performed at the materials research center (MRC) Malviya National Institute of Technology, MNIT Jaipur, and the experimental setup is shown in Figure 3.17.

Figure 3.17: Experimental system for FESEM (Source: MRC, MNIT, Jaipur)

3.2.4 Transmission Electron Microscopy

Transmission electron microscopy (TEM) is a major analytical tool widely used in the physical and biological sciences, including various researches like material science, nanotechnology, virology, and cancer research. The working of TEM is similar to the projector system except that a beam of electrons shines on the sample instead of light [Zhang *et al.*, 2008]. The transmitted part of the electron beam is projected onto a screen for visualization purposes. The schematic representation is shown in Figure 3.18, indicates the working and instrument part of the TEM system [Zhang *et al.*, 2008].

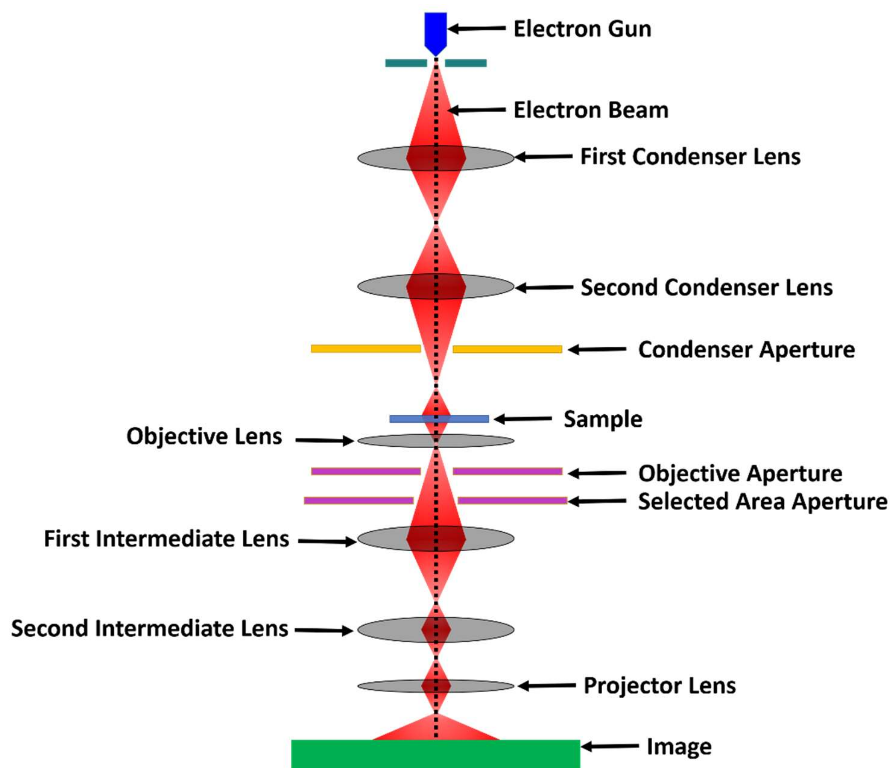

Figure 3.18: Schematic representation of the working and instrumentation part of the TEM system

The TEM instrumentation consists of an electron gun, lens systems including condenser lens, objective lens, intermediate lens and projector lens, sample holder, and imaging or visualizing system. Here, the electron gun works similarly to the cathode ray tube. The electron beam has become highly focused by condenser lenses and apertures while leaving the electron gun. The combination of condenser lenses and apertures permits only a specific energy range of electrons to pass; thus, the electrons with definite energy fall on the sample. The sample holder contains a mechanical arm for holding the sample and is also utilized for position control. The imaging or visualizing system possesses another set of electromagnetic lenses, which has a set of intermediate lens and projector lens, which helps to make the image on the screen [Zhang *et al.*, 2008]. The screen is made up of a phosphorescent plate, shines by striking the electrons.

3.2.5 Raman Spectroscopy

Raman Spectroscopy is a technique used to determine vibrational rotational and low-frequency modes of molecules. The working of Raman spectroscopy depends on the inelastic scattering of photons, also called Raman scattering. This scattering defines the Raman active modes[Downes and Elfick, 2010].

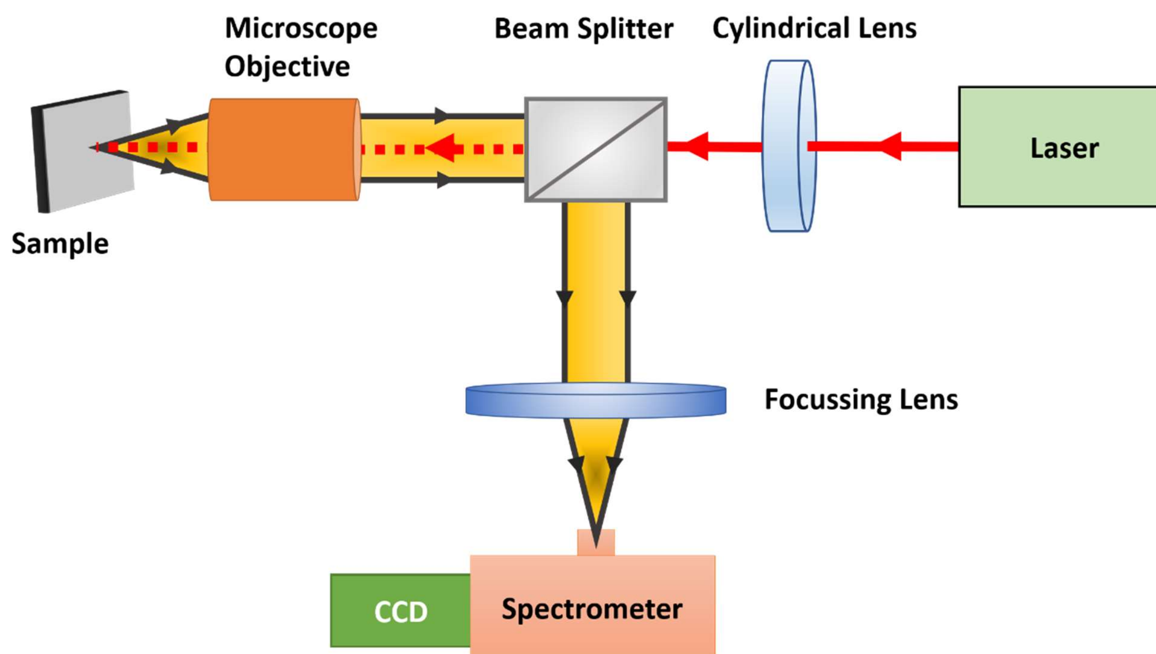

Figure 3.19: Working of Raman spectroscopy

Figure 3.19 shows the schematic representation of the Raman spectroscopy. Here, a monochromatic laser, usually in the visible or near-infrared range, is utilized is passed through a cylindrical lens. When the laser interacts with the sample, the molecular vibrations, phonons, or other type of excitation happens, results in the variation of the laser energy; thus, this energy shift of laser, also called Raman-shifted light, is filtered by a beam splitter mirror and scattered [Downes and Elfick, 2010]. This scattered light is focused by a focusing lens and directed towards the spectrometer. The spectrometer is connected with the CCD detector to analyze the spectra.

3.2.6 Atomic Absorption Spectroscopy

Atomic absorption spectroscopy (AAS) is one of the most commonly used techniques in chemical laboratories. This method has the capability to identify about 70 different elements in the solution [Kumar and Whitesides, 1993]. This technique and its principle were given for the first time by Kirchhoff and Bunsen in the 1860s. However, its practical implementations and utilization as an analytical approach were revealed in 1955 [Chow *et al.*, 2005]. The principle of

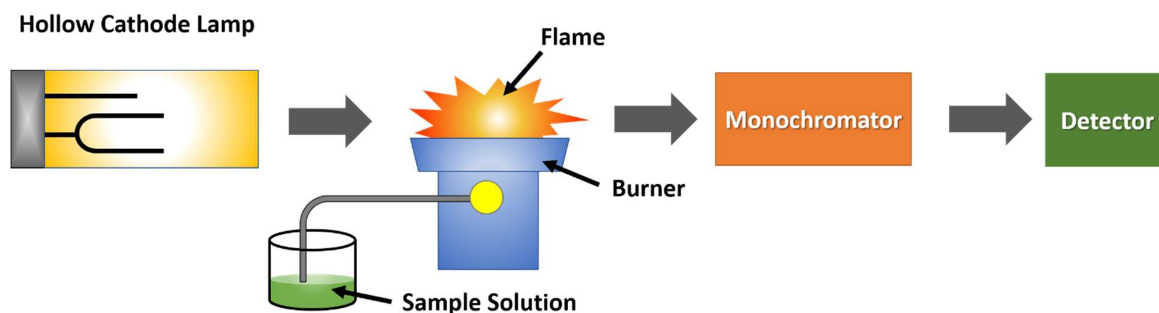

Figure 3.20: Schematic representation of Atomic Absorption Spectroscopy

AAS is very simple as it utilizes light absorption to determine the concentration of atoms and ions in a solution.

Figure 3.20 depicts the schematic representation of the process of an atomic absorption spectrometer. In this process, a specific wavelength of light was produced by the light source. Further, electrothermal or flame atomization is utilized for the introduction of the sample and analyte atomization. The corresponding light is directed towards a monochromator as a particular element emits the particular light, and the detector detected the changes. Figure 3.21 shows the system utilized for AAS measurement at MRC, MNIT Jaipur.

Figure 3.21: Atomic Absorption Spectroscopy system for elemental analysis of solutions (Source: MRC, MNIT Jaipur)

3.2.7 Inductively Coupled Plasma- Mass Spectroscopy

Inductively Coupled Plasma Mass Spectrometry (ICP-MS) is one of the most powerful tools for the elemental analysis in a solution. This technique was announced commercially in 1983 and has become widely accepted. The ICP-MS has excellent detection capabilities, especially for the rare-earth elements. This method comprises a high-temperature ICP source along with a mass spectrometer, which ionizes the desired elements in the sample. After ionization, the ions are then separated and identified by the mass spectrometer. Figure 3.22(a) depicts a schematic representation of the ICP-MS. In this work, the ICP-MS was carried out in Central Research

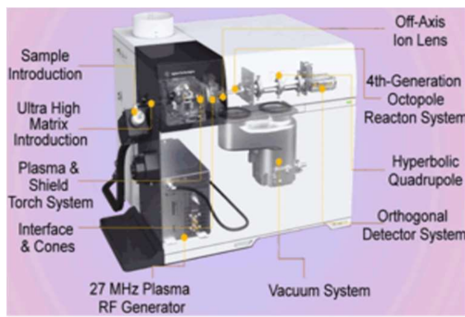

(a) (b)

Figure 3.22: (a) Schematic representation of ICP-MS (b) ICP-MS System for detection of ionic concentration (Source: CRF, IIT Delhi)

Facility, Indian Institute of Technology Delhi (CRF, IIT Delhi), for the elemental analysis. The system utilized in this work has been shown in Figure 3.22(b).

3.2.8 Electrical Characterization Process

In this work, the electrical characterization process was carried out on AlGaN/GaN HEMT devices. This process was carried out using a microscopic probe station where three probes were utilized for the measurement of I-V characteristics of the device. These characteristics include I_D-V_D and I_D-V_G measurements. While preparing AlGaN/GaN HEMT as a sensor for heavy metal ion detection, two probes utilized for sensing, and drain current versus time characteristics were observed. Here, the probe station was connected to the source meter of the Keithley-4200 semiconductor characterization system (SCS), which observes the electrical properties of the device in different modes such as voltage sweep, current sweep, voltage bias, and current bias and stores it. It also provides a very simple user interface installed on Windows operating system. Figure 3.23 demonstrates the system utilized for electrical characterization at IIT Jodhpur.

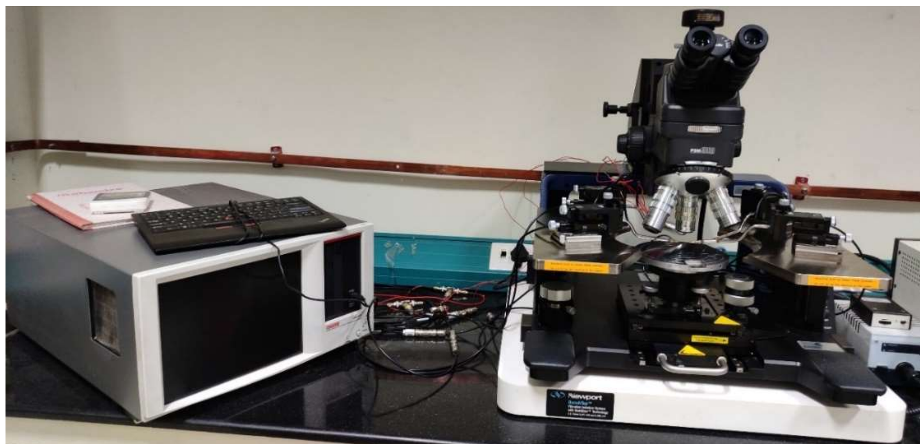

Figure 3.23: Probe station with Keithley-4200 SCS for electrical characterization at IIT Jodhpur.

3.3 CONCLUSION

In this chapter, various fabrication and characterization techniques were described, along with their principles and working. All these methods were utilized somewhere in the thesis for different analyses, which can be seen in the next chapters.

…